



Received on 19 December 2019; received in revised form, 04 April 2020; accepted, 11 April 2020; published 01 December 2020

## SYNTHESIS, CHARACTERIZATION AND BIOLOGICAL STUDIES OF RUTHENIUM (II) COMPLEXES OF SUBSTITUTED 2-{4, 5-BIS[(E)-2-PHENYLETHENYL]-1H-IMIDAZOL-2-YL}-1H-BENZIMIDAZOLE

M. Kiruthika <sup>\*1</sup>, R. Elayaperumal <sup>2</sup> and C. Hariharan <sup>3</sup>

Department of Chemistry <sup>1</sup>, Arignar Anna Government Arts College, Musiri, Trichy - 621211, Tamil Nadu, India.

Department of Chemistry <sup>2</sup>, Paavai Engineering College, Namakkal - 637018, Tamil Nadu, India.

Department of Physics <sup>3</sup>, Jamal Mohamed College, Tiruchirappalli - 620020, Tamil Nadu, India.

### Keywords:

Benzimidazole, Ruthenium(II), MCF7, DNA cleavage

### Correspondence to Author:

**Dr. M. Kiruthika**

Assistant Professor,  
Department of Chemistry,  
Arignar Anna Government Arts  
College, Musiri, Trichy - 621211,  
Tamil Nadu, India.

**E-mail:** kumarikiruthika@gmail.com

**ABSTRACT:** Ruthenium(II) complexes of the type [Ru(bpy) 2(L)](PF6)2, where L= 2-{4,5-bis[(E)-2-phenylethenyl]-1H-imidazol-2-yl}-1H-benzimidazole (1), 2-{4,5-bis[(E)-2-(4-chlorophenyl)ethenyl]-1H-imidazol-2-yl}-1H-benzimidazole (2), 2-{4,5-bis[(E)-2-(4-fluorophenyl) ethenyl]-1H-imidazol-2-yl} -1H-benzimidazole (3), 2-{4,5-bis[(E)-2-(4-methylphenyl) ethenyl]-1H-imidazol-2-yl}-1H-benzimidazole (4), 2-{4,5-bis[(E)-2-(4-methoxyphenyl) ethenyl]-1H-imidazol-2-yl}-1H-benzimidazole (5) have been synthesized and characterized by elemental analyses and spectral (IR, UV-vis, NMR, ESI-MS) techniques. The redox behavior of the complexes has been studied by cyclic and differential pulse voltammetry. In acetonitrile solution, all the complexes exhibit characteristic metal to ligand charge transfer (MLCT) absorptions and ligand-based transitions. The complexes showed efficient DNA cleavage activity in the presence of light at the wavelength of 480 nm. The complexes are also able to cleave supercoiled pUC19 plasmid DNA *via* guanine base oxidation in a concentration-dependent manner. *In-vitro* cytotoxic activity of the complexes shows that complex 1 has better anticancer activity against MCF7 human breast cancer cells with an IC<sub>50</sub> value of 7.9 μM. The antimicrobial activities of the ligand and their metal complexes were screened by agar diffusion method and found that the metal complexes have higher antimicrobial activity than the free ligand.

**INTRODUCTION:** Throughout the previous three decades, anticancer chemotherapy has focused on cisplatin derivatives. Regardless of their predictable reactions, cisplatin derivatives have a focal part in most anticancer treatments <sup>1</sup>. A large number of platinum compounds have been combined, trying to defeat the issues of cisplatin.

Incredibly none of these has possessed the capacity to supplant cisplatin in routine chemotherapy medicines. In the look for medications with cutting edge clinical viability, decreased harmfulness, and a more extensive range of action, metals other than platinum, for example, rhodium and ruthenium, have been considered.

Non-platinum active compounds are having different mechanisms of action and bio-distribution so that they are found to be active against human malignancies. Because of a less toxic nature, ruthenium complexes are found to be superior to cisplatin. Ruthenium has found its way into the clinic, where its properties are exploited for very

<p><b>QUICK RESPONSE CODE</b></p>	<p><b>DOI:</b> 10.13040/IJPSR.0975-8232.11(12).6550-60</p> <hr/> <p>The article can be accessed online on <a href="http://www.ijpsr.com">www.ijpsr.com</a></p> <hr/> <p>DOI link: <a href="http://dx.doi.org/10.13040/IJPSR.0975-8232.11(12).6550-60">http://dx.doi.org/10.13040/IJPSR.0975-8232.11(12).6550-60</a></p>
-----------------------------------	---

miscellaneous uses. The radiophysical properties of  $^{97}\text{Ru}$  can be connected to radiodiagnostic imaging <sup>2, 3</sup>. Other ruthenium compounds have potential as immunosuppressants (cis-[Ru (III) (NH<sub>3</sub>)<sub>4</sub> (HIm) 2]<sup>3+</sup>), antimicrobials ([Ru (II) Cl<sub>2</sub> (chloroquine)<sub>2</sub>]), antibiotics, antioxidants, vasodilator / vasoconstrictor agents and, as previously mentioned, as drugs for cancer chemotherapy <sup>4</sup>. The ligand-exchange kinetics of ruthenium (II) and ruthenium (III) complexes have been observed to be like those of platinum (II) complexes. This property makes them the first choice in the search for compounds that exhibit similar biological effects to platinum (II) drugs <sup>5</sup>.

The scope of available oxidation states of ruthenium under physiological conditions makes this metal novel among the platinum compounds. The ruthenium compounds, prevalently octahedral, can be Ru (II), Ru (III), or Ru (IV). Ru (III) compounds have a tendency to be more biologically inert compared to Ru (II) and Ru (IV) complexes <sup>6</sup>. The redox capability of ruthenium compounds can be exploited to enhance the viability of Ru-based medications in the clinic <sup>5, 6</sup>. The passage of two Ru(III) based drugs, NAMI-A ([H<sub>2</sub>Im]{trans-[Ru (III) Cl<sub>4</sub> (dmsO) (imidazole)]})<sup>7</sup> and KP1019 (trans-[RuCl<sub>4</sub> (indazole)<sub>2</sub>]-)<sup>8</sup> into clinical trials for the treatment of metastatic tumors expanded the enthusiasm for this metal.

Additionally, more number of Ru (II) compounds are being synthesized to show the cytotoxic and antitumor properties <sup>9, 10</sup> and are presently under dynamic examination. Benzimidazoles are important group of heterocyclic compounds that are naturally active and of noteworthy significance in therapeutic chemistry. The derivatives of benzimidazoles have been of huge enthusiasm to medicinal chemistry since its substituents had different biological activities, for example, antioxidant <sup>11</sup>, antimicrobial <sup>12</sup>, anticancer <sup>13</sup>, and anti-inflammatory <sup>14</sup> activities. All benzimidazole subordinates with their two-ring frameworks bear distinctive useful substituents, and this prompts basic alteration of the physico-chemical, pharmacokinetic and metabolic properties of these drugs. In the previous couple of decades, benzimidazole and its derivatives have received much consideration because of their chemotherapeutic properties. Since, the metal ion, its oxidation state, and

chelating ligand circle assume imperative parts in deciding chemical and biological properties, a series of Ru (II) compounds encasing benzimidazole based ligands have been synthesized and structurally characterized. All the complexes have been subjected to biological studies such as DNA photocleavage, antioxidant, antimicrobial, and cyto-toxic activity testing as DNA photocleavage, anti-microbial and cytotoxic activity testing.

## EXPERIMENTAL:

**MATERIALS AND METHODS:** Ruthenium chloride trihydrate, ammonium hexafluoro phosphate, 4-chlorobenzaldehyde, 4-fluoro-benzaldehyde, 4-methyl benzaldehyde, 4-methoxy benzaldehyde and benzaldehyde were purchased from Sigma-Aldrich. Benzimidazole- 2-carboxaldehyde was prepared by following a reported procedure <sup>15</sup>. Acetic acid, ammonium acetate, methanol, acetonitrile, and ethanol were purchased from SD Fine chemicals.

Absorption spectra were recorded on Shimadzu UV-160A UV-Visible spectrophotometer. Cyclic (CV) and differential pulse voltammetry (DPV) were performed by using CH instrument (USA) model CH-620 B electrochemical analyzer. A conventional three-electrode system consisting of the platinum disc as a working electrode, platinum wire as an auxiliary electrode, and saturated calomel (SCE) as a reference electrode was used for the electrochemical measurements. 0.1 M tetrabutylammonium perchlorate (TBAP) was used as the supporting electrolyte for all the experiments. Positive ion electrospray ionization mass spectra of the complexes were obtained by using Thermo Finnigan LCQ 6000 advantage max ion trap mass spectrometer. Elemental analyses were performed using Carlo Erba 1108 analyzer at Cochin University. IR spectra were recorded as KBr pellets in the 400-4000 cm<sup>-1</sup> region using a Shimadzu FT-IR 8000 spectrophotometer. All the DNA gel images were taken using UVITEC gel documentation system, and fragments were analyzed using UVI chem and UVI-band software.

**Synthesis of Ligands:** The ligands (1E, 5E)-1, 6-diphenylhexa-1, 5-diene-3, 4-dione, (1E, 5E)-1, 6-bis (4-chlorophenyl) hexa-1, 5-diene-3, 4-dione, (1E, 5E)-1, 6-bis (4-fluorophenyl) hexa-1, 5-diene-3, 4-dione, (1E, 5E)-1, 6-bis(4-methylphenyl)hexa-

1, 5-diene-3, 4-dione and (1E, 5E)-1, 6-bis(4-methoxyphenyl) hexa-1, 5-diene-3, 4-dione were prepared as reported elsewhere<sup>16</sup>.

**Synthesis of 2-{4, 5-bis[(E)-2-phenylethenyl]-1H-imidazol-2-yl}-1H-benzimidazole (L1):** (1E, 5E)-1,6-diphenylhexa-1, 5-diene-3, 4-dione (0.5 g, 1.91 mmol), benzimidazole-2- carboxaldehyde (0.29 g, 2.00 mmol) and ammonium acetate (4 g, 50 mmol) were dissolved in 30 mL acetic acid and heated to reflux for 3 h. After cooling, cold water (20 mL) was added to the solution, during which reddish brown precipitate appeared. It was filtered and purified by column chromatography on silica gel using ethyl acetate:hexane (1:4) as an eluent (Yield: 0.416 g, 56%). ESI-MS: m/z (relative intensity): 389.9 (M+1)<sup>+</sup>.  $\delta_H$  (400 MHz; DMSO-d<sub>6</sub>; Me<sub>4</sub>Si) 7.29(4H, t, J=2.8 Hz), 7.21(4H, t, J=3.2 Hz), 7.18(4H, d, J=4.0 Hz), 7.31(4H, d, J=5.2 Hz), 7.71 (2H, d, J=2.8 Hz), 7.26(2H, t, J=7.6 Hz), 12.22(2H, s); Anal. Calc. for C<sub>26</sub>H<sub>20</sub>N<sub>4</sub>: C, 80.91; H, 5.19; N, 14.42. Found: C, 80.88; H, 5.17; N, 14.38; IR, cm<sup>-1</sup> (KBr pellet) 3423, 2313, 1545, 1271, 745, 696; UV-Visible  $\lambda_{max}$ , nm ( $\epsilon$ , M<sup>-1</sup> cm<sup>-1</sup>) 313(16000), 282(49314).

**Synthesis of 2-{4, 5-bis[(E)-2-(4-chlorophenyl)ethenyl]-1H-imidazol-2-yl}-1H benzimidazole (L2):** An analogous synthetic procedure using (1E, 5E)-1, 6-bis(4-chlorophenyl)hexa-1, 5-diene-3, 4-dione (0.5 g, 1.51 mmol) instead of (1E, 5E)-1, 6-diphenylhexa-1, 5-diene-3,4-dione was used to prepare 2-{4,5-bis[(E)-2-(4-chlorophenyl)ethenyl]-1H-imidazol-2-yl}-1H-benzimidazole (Yield: 0.438 g, 61%). ESI-MS: m/z (relative intensity): 458.1 (M+1)<sup>+</sup>.  $\delta_H$  (400 MHz; DMSO-d<sub>6</sub>; Me<sub>4</sub>Si) 7.32 (4H, d, J=2.8 Hz), 7.34(4H, d, J=3.2 Hz), 7.29 (4H, d, J=2.8 Hz), 7.71(2H, d, J=2.4 Hz), 7.30 (2H, t, J=1.6 Hz), 12.42(2H, s); Anal. Calc. for C<sub>26</sub>H<sub>18</sub>Cl<sub>2</sub>N<sub>4</sub>: C, 68.28; H, 3.97; N, 12.25. Found: C, 68.25; H, 3.95; N, 12.22; IR, cm<sup>-1</sup> (KBr pellet) 3417, 2312, 1606, 1489, 743, 419; UV-Visible  $\lambda_{max}$ , nm ( $\epsilon$ , M<sup>-1</sup> cm<sup>-1</sup>) 339(15145), 285 (49430).

**Synthesis of 2-{4,5-bis[(E)-2-(4-fluorophenyl)ethenyl]-1H-imidazol-2-yl}-1H benzimidazole (L3):** The same method was adopted using (1E, 5E)-1, 6-bis(4-fluorophenyl)hexa-1, 5-diene-3, 4-dione (0.5 g, 1.68 mmol) instead of (1E, 5E)-1, 6-bis (4-chlorophenyl)hexa-1, 5-diene-3, 4-dione was used to prepare -{4, 5-bis[(E)-2- (4-fluorophenyl)

ethenyl]-1H- imidazol-2-yl}- 1H-benzimidazole (Yield: 0.371 g, 52%). ESI-MS: m/z (relative intensity): 425.2 (M+1)<sup>+</sup>.  $\delta_H$  (400 MHz; DMSO-d<sub>6</sub>; Me<sub>4</sub>Si) 7.18(4H, d, J=5.2 Hz), 7.24(4H, d, J=6.0 Hz), 7.11(4H, d, J=6.8 Hz), 7.31(4H, d, J=5.2 Hz), 7.71(2H, d, J=7.2 Hz), 7.32(2H, t, J=2.8 Hz), 12.72(2H, s); Anal. Calc. for C<sub>26</sub>H<sub>18</sub>F<sub>2</sub>N<sub>4</sub>: C, 73.57; H, 4.27; N, 13.20. Found: C, 73.55; H, 4.26; N, 13.16; IR, cm<sup>-1</sup> (KBr pellet) 3398, 2924, 1601, 1506, 1230, 839, 428; UV-Visible  $\lambda_{max}$ , nm ( $\epsilon$ , M<sup>-1</sup> cm<sup>-1</sup>) 326(17265), 282(46590).

**Synthesis of 2-{4,5-bis[(E)-2-(4-methylphenyl)ethenyl]-1H-imidazol-2-yl}-1H-benzimidazole (L4):** While preparing 2-{4, 5-bis[(E)-2-(4-methylphenyl) ethenyl]- 1H-imidazol- 2-yl}-1H-benzimidazole, (1E, 5E)-1, 6-bis(4- methylphenyl) hexa-1, 5-diene-3, 4-dione (0.5 g, 1.72 mmol) was used in place of (1E,5E)-1, 6-bis(4-fluorophenyl) hexa-1, 5-diene-3, 4-dione. A brown precipitate was appeared. It was filtered and purified by column chromatography on silica using ethyl acetate: hexane (1:4) as an eluent. (Yield 0.52 g, 72%). ESI-MS: m/z (relative intensity): 417.1 (M+1)<sup>+</sup>.  $\delta_H$  (400 MHz; DMSO-d<sub>6</sub>; Me<sub>4</sub>Si) 7.08 (4H, d, J=3.2 Hz), 7.10(4H, d, J=3.2 Hz), 6.97 (4H, d, J=6.8 Hz), 7.59(2H, d, J=2.0 Hz), 7.10 (2H, t, J=3.2 Hz), 2.24(6H, s), 12.42(2H, s); Anal. Calc. for C<sub>28</sub>H<sub>24</sub>N<sub>4</sub>: C, 80.74; H, 5.81; N, 13.45. Found: C, 80.72; H, 5.78; N, 13.43; IR, cm<sup>-1</sup> (KBr pellet) 3417, 2922, 1607, 1513, 1272, 742, 424; UV-Visible  $\lambda_{max}$ , nm ( $\epsilon$ , M<sup>-1</sup> cm<sup>-1</sup>) 323(17475), 283 (46090).

**Synthesis of 2-{4,5-bis[(E)-2-(4-methoxyphenyl)ethenyl]-1H-imidazol-2-yl}-1H-benzimidazole (L5):** An analogous synthetic procedure using (1E, 5E)-1, 6-bis(4-methoxyphenyl)hexa-1,5-diene-3,4-dione (0.5 g, 1.55 mmol) instead of (1E,5E)-1, 6-bis (4-methylphenyl) hexa-1, 5-diene-3, 4-dione was used to prepare 2-{4, 5-bis[(E)-2 -(4-methoxyphenyl) ethenyl]-1H-imidazol-2-yl}-1H-benzimidazole. (Yield 0.33 g, 47%). ESI-MS: m/z (relative intensity): 449.1 (M)<sup>+</sup>.  $\delta_H$  (400 MHz; DMSO-d<sub>6</sub>; Me<sub>4</sub>Si) 6.77(4H, d, J=3.2 Hz), 7.29 (4H, d, J=3.2 Hz), 7.01(4H, d, J=2.0 Hz), 7.71 (2H, d, J=2.8 Hz), 7.28(2H, t, J=2.8 Hz), 3.78 (6H, s), 12.41(2H, s); Anal. Calc. for C<sub>28</sub>H<sub>24</sub>O<sub>2</sub>N<sub>4</sub>: C, 74.98; H, 5.39; N, 12.49. Found: C, 74.95; H, 5.37; N, 12.44; IR, cm<sup>-1</sup> (KBr pellet) 3451, 2312, 1607,

1508, 1249, 833, 586; UV-Visible  $\lambda_{\max}$ , nm ( $\epsilon$ ,  $M^{-1} \text{ cm}^{-1}$ ) 315(16495), 284 (46805).

### Synthesis of Ruthenium (II) Complexes:

**Synthesis of [Ru(bpy)<sub>2</sub>(L1)](PF<sub>6</sub>)<sub>2</sub> (1):** A mixture of [cis-Ru(bpy)<sub>2</sub>Cl<sub>2</sub>] $\cdot$ 2H<sub>2</sub>O<sub>17</sub> (0.2 g, 0.38 mmol) and L1 (0.149 g, 0.38 mmol) was suspended in an ethanol/water solvent mixture (3/1, v/v). The mixture was refluxed under an inert atmosphere for 4 h while vigorous stirring was maintained. The reaction mixture was cooled to room temperature; the solvent was reduced under vacuum to one-third of its initial volume. A saturated aqueous solution of NH<sub>4</sub>PF<sub>6</sub> was added to precipitate [Ru (bpy)<sub>2</sub>(L1)]<sup>2+</sup> as its hexafluorophosphate salt. The product was filtered and washed with water (3  $\times$  10 mL) and dried. Yield: 0.34 g, 81%. Anal. Calc. for C<sub>46</sub>H<sub>36</sub>F<sub>12</sub>N<sub>8</sub>P<sub>2</sub>Ru: C, 50.60; H, 3.32; N, 10.26. Found: C, 50.58; H, 3.28; N, 10.25. ESI-MS: m/z 946.0 (M – PF<sub>6</sub>)<sup>+</sup>; IR, cm<sup>-1</sup> (KBr pellet) 3716, 2363, 1516, 845; UV-Visible  $\lambda_{\max}$ , nm ( $\epsilon$ ,  $M^{-1} \text{ cm}^{-1}$ ) 464 (8700), 343 (20950), 290 (53750), 242 (43450).

**Synthesis of [Ru(bpy)<sub>2</sub>(L2)](PF<sub>6</sub>)<sub>2</sub> (2):** The synthesis and purification of compound 2 were similar to those of 1 using [Ru(bpy)<sub>2</sub>Cl<sub>2</sub>] $\cdot$ 2H<sub>2</sub>O (0.2 g, 0.38 mmol) and L2 (0.17 g, 0.38 mmol). Yield: 0.366 g, 83%, Anal. Calc. for C<sub>46</sub>H<sub>34</sub>C<sub>12</sub>F<sub>12</sub>N<sub>8</sub>P<sub>2</sub>Ru: C, 47.60; H, 2.95; N, 9.65. Found: C, 47.57; H, 2.93; N, 9.62; ESI-MS: m/z 435.4 (M – 2PF<sub>6</sub>)<sup>2+</sup>; IR, cm<sup>-1</sup> (KBr pellet) 3717, 3047, 2363, 1516, 844; UV-Visible  $\lambda_{\max}$ , nm ( $\epsilon$ ,  $M^{-1} \text{ cm}^{-1}$ ) 462(7400), 346(19350), 292(52350), 244 (43400).

**Synthesis of [Ru(bpy)<sub>2</sub>(L3)](PF<sub>6</sub>)<sub>2</sub> (3):** This compound was synthesized and purified by a procedure similar to that described for compound 1, except L3 (0.16 g, 0.38 mmol) was used instead of L2. Yield: 0.368 g, 86%, Anal. Calc. for C<sub>46</sub>H<sub>34</sub>F<sub>14</sub>N<sub>8</sub>P<sub>2</sub>Ru: C, 48.99; H, 3.04; N, 9.94. Found: C, 48.95; H, 3.01; N, 9.92; ESI-MS: m/z 419.1 (M – PF<sub>6</sub>)<sup>2+</sup>; IR, cm<sup>-1</sup> (KBr pellet) 3726, 3608, 1602, 1510, 1454, 1230, 763; UV-Visible  $\lambda_{\max}$ , nm ( $\epsilon$ ,  $M^{-1} \text{ cm}^{-1}$ ) 463(7500), 338(19350), 291 (47850), 242(40200).

**Synthesis of [Ru(bpy)<sub>2</sub>(L4)](PF<sub>6</sub>)<sub>2</sub> (4):** This complex was prepared by adopting the procedure used for the isolation of 3 but by using L4 (0.16 g, 0.38 mmol) instead of L3. Yield: 0.349 g, 82%.

Anal. Calc. for C<sub>48</sub>H<sub>40</sub>F<sub>12</sub>N<sub>8</sub>P<sub>2</sub>Ru: C, 51.48; H, 3.60; N, 10.01. Found: C, 51.45; H, 3.58; N, 9.97. ESI-MS: m/z 487.3 (M – 2PF<sub>6</sub>)<sup>+</sup>; IR, cm<sup>-1</sup> (KBr pellet) 3728, 2920, 2308, 1514, 843, 416; UV-Visible  $\lambda_{\max}$ , nm ( $\epsilon$ ,  $M^{-1} \text{ cm}^{-1}$ ) 466(8550), 344 (21450), 290 (53900), 244 (43250).

**Synthesis of [Ru (bpy)<sub>2</sub>(L5)](PF<sub>6</sub>)<sub>2</sub> (5):** The synthesis and purification of compound 5 were similar to those of 4 using [Ru(bpy)<sub>2</sub>Cl<sub>2</sub>] $\cdot$ 2H<sub>2</sub>O (0.2 g, 0.38 mmol) and L5 (0.17 g, 0.38 mmol). Yield: 0.372 g, 85%, Anal. Calc. for C<sub>48</sub>H<sub>40</sub>O<sub>2</sub>F<sub>12</sub>N<sub>8</sub>P<sub>2</sub>Ru: C, 50.05; H, 3.50; N, 9.73. Found: C, 50.02; H, 3.47; N, 9.71; ESI-MS: m/z 430.2 (M – 2PF<sub>6</sub>)<sup>2+</sup>; IR, cm<sup>-1</sup> (KBr pellet) 3701, 2362, 1695, 1516, 1250, 842; UV-Visible  $\lambda_{\max}$ , nm ( $\epsilon$ ,  $M^{-1} \text{ cm}^{-1}$ ) 470(8850), 332(24900), 289(59600), 245(41300).

**DNA Cleavage Activity:** Photonuclease activity of the complexes was monitored using gel electrophoresis of plasmid DNA (pUC19). The solutions were prepared for the photolysis experiment containing 3  $\mu$ L of 100  $\mu$ g mL<sup>-1</sup> plasmid DNA in Tris buffer and varying amounts of complexes 1- 5 (0–48  $\mu$ M). Each solution was incubated for 1 hour and then irradiated at 450 nm for various time intervals varying from 10 min to 60 min.

The samples were then subjected to electrophoresis in 0.8% agarose gel (tris-boric acid-EDTA buffer, pH 8.0) at 50 V for 2 h. The gel was stained with 0.5  $\mu$ g mL<sup>-1</sup> of ethidium bromide. The stained gel was illuminated under a UV lamp and gel documented. In a separate experiment, the DNA was incubated with 48  $\mu$ M of the metal complex and 10 mM of histidine and irradiated at 440 nm. The photolyzed solution was subsequently subjected to electrophoresis.

**In-vitro Anticancer Assay:** 3-[4, 5-dimethylthiazol-2-yl] 2, 5-diphenyltetrazolium bromide (MTT) is a yellow water-soluble tetrazolium salt. A mitochondrial enzyme in living cells, succinate-dehydrogenase, cleaves the tetrazolium ring, converting the MTT to an insoluble purple formazan.

Therefore, the amount of formazan produced is directly proportional to the number of viable cells.

The human breast cancer cell line (MCF 7) was obtained from National Centre for Cell Science (NCCS), Pune and grown in Eagles Minimum Essential Medium (EMEM) containing 10% fetal bovine serum (FBS). All cells were maintained at 37 °C, 5% CO<sub>2</sub>, 95% air and 100% relative humidity. For screening experiments, the cells were seeded into 96-well plates in 100 mL of the respective medium containing 10% FBS, at a plating density of 10 000 cells / well and incubated at 37 °C, 5% CO<sub>2</sub>, 95% air and 100% relative humidity for 24 h prior to the addition of compounds. The compounds were dissolved in DMSO and diluted in the respective medium containing 1% FBS. After 24 h, the medium was replaced with the respective medium with 1% FBS containing the compounds at various concentrations and incubated at 37 °C, 5% CO<sub>2</sub>, 95% air and 100 % relative humidity for 48 h. Experiments were performed in triplicate and the medium without the compounds served as control. After 48 h, 15 µL of MTT (5 mg mL<sup>-1</sup>) in phosphate buffered saline (PBS) was added to each well and incubated at 37 °C for 4 h. The medium with MTT was then removed, and the formed formazan crystals were dissolved in 100 mL of DMSO, and the absorbance measured at 570 nm using a micro plate reader. The % cell inhibition was determined using the following formula, and a graph was plotted between % of cell inhibition and concentration. From this plot, the IC<sub>50</sub> value was calculated. The % cell inhibition was determined using the following formula.

$$\% \text{ Cell Inhibition} = 100 - \frac{\text{Abs (sample)}}{\text{Abs (control)}} \times 100$$

A nonlinear regression graph was plotted between % Cell inhibition and Log concentration, and IC<sub>50</sub> was determined using GraphPad Prism software.

**Antimicrobial Assay:** Test Microorganisms: A gram-positive bacteria (*Staphylococcus aureus*), gram-negative bacteria (*Escherichia coli*), and one Yeast *Candida albicans* were used in the present study for evaluation of antimicrobial activity of the synthesized compounds. The medium used for the antimicrobial testing was Muller Hilton agar media and autoclaved at 15 lbs/in 2 for 15 min.

Antimicrobial Activity: Agar disc diffusion method was used to study the antimicrobial activity of the newly synthesized compounds<sup>18,19</sup>.

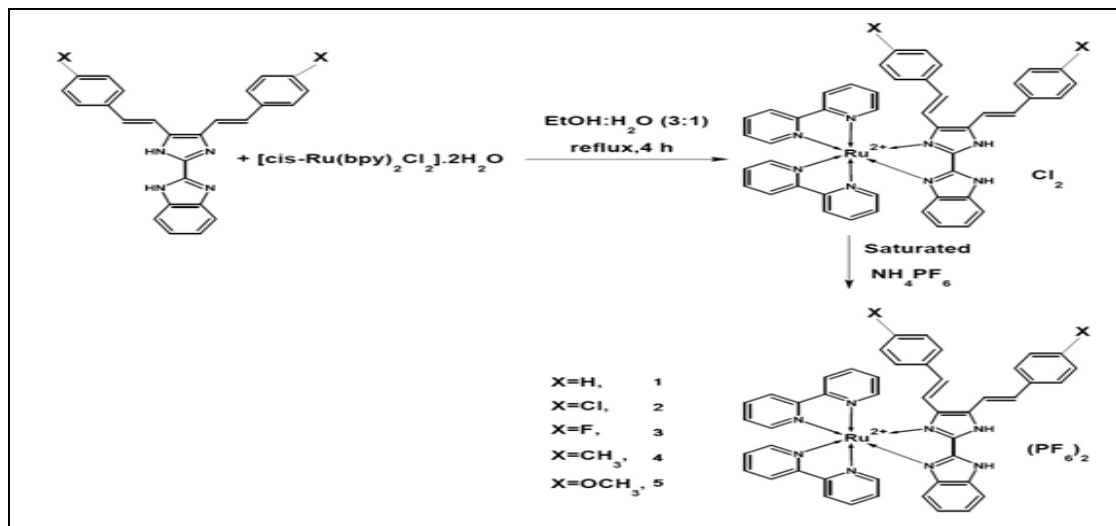
For the evaluation of antimicrobial activity, the size of inoculums was adjusted to approximately 108 colony-forming units (cfu/mL) by suspending the culture in sterile distilled water. Petri dishes containing 20 mL of Muller Hilton agar medium were swabbed with a culture of the respective microbial strains and kept for 15 min for the absorption of culture. Sterile borer is used to create the wells (6 mm in diameter), and we added 25, 50, and 100 µL solution of each compound of 25, 50, and 100 µg/mL concentration respectively re-constituted in the DMSO on the preinoculated plates. All the plates were incubated at 37 °C for 24 hrs. Antimicrobial activity of all the synthesized compounds was determined by measuring the zone of inhibition around the wells. DMSO was used as a negative control, whereas Gentamycin was used as a positive control. This procedure was performed in three replicate plates for each organism.

## RESULTS AND DISCUSSION:

**Synthesis and Characterization:** The complexes are prepared in high yield by following a general procedure in which [Ru(bpy)<sub>2</sub>Cl<sub>2</sub>] $\cdot$ 2H<sub>2</sub>O was reacted with the newly synthesized ligands (L1-L5) in an aqueous ethanolic medium. The synthesized complexes **Fig. 1** have been isolated as their hexa-fluorophosphate salts and characterized by various techniques such as FT-IR, UV-Visible, ESI-MS, elemental analyses, cyclic and differential pulse voltammetries. The synthesized ligands and complexes are stable at room temperature and non-hygroscopic. The analytical data **Table 1** obtained for these complexes are in good agreement with the proposed molecular formulae. The mass spectra of the complexes [Ru(bpy)<sub>2</sub>(L1)](PF<sub>6</sub>)<sub>2</sub>, [Ru(bpy)<sub>2</sub>(L2)](PF<sub>6</sub>)<sub>2</sub>, [Ru(bpy)<sub>2</sub>(L3)](PF<sub>6</sub>)<sub>2</sub>, [Ru(bpy)<sub>2</sub>(L4)](PF<sub>6</sub>)<sub>2</sub> and [Ru(bpy)<sub>2</sub>(L5)](PF<sub>6</sub>)<sub>2</sub> displayed base peaks at 946.0, 435.39, 419.07, 487.33 and 430.17 respectively. These peaks are reliable with the proposed molecular formulae of the corresponding ruthenium (II) complexes. The electronic spectra of all the complexes were recorded in acetonitrile, and the results are listed in **Table 1**. Representative spectra of the complexes (1-5) are shown in **Fig. 2**. If the field around Ru<sup>2+</sup> is assumed as octahedral, the ground state of ruthenium (II) (t<sub>2g</sub><sup>6</sup> configuration) should be 1A<sub>1g</sub>. The excited states corresponding to t<sub>2g</sub><sup>5</sup>e<sub>g</sub><sup>1</sup> configuration are 3T<sub>1g</sub>, 3T<sub>2g</sub>, 1T<sub>1g</sub>, and 1T<sub>2g</sub> in increasing order of energy.

Thus, four bands corresponding to the transitions from  $1A_{1g}$  to  $3T_{1g}$ ,  $3T_{2g}$ ,  $1T_{1g}$ , and  $1T_{2g}$  should appear in the electronic spectra of the complexes.

In the low spin  $d^6$  system, no band due to ligand to metal charge transfer transitions is possible in the visible region<sup>20</sup>.



Each complex shows broadband in the region of 462-470 nm. Based on the values of molar extinction coefficient ( $7400-8850 \text{ M}^{-1} \text{ cm}^{-1}$ ), this band has been assigned to charge transfer transitions occurring from excitation of an electron from metal  $t_{2g}$  level to unfilled molecular orbitals derived from the  $\pi^*$  level of the ligands<sup>21</sup>. The  $\lambda_{\text{max}}$  value for the well-defined lowest energy band illustrates a clear trend of increasing as the coligand (L1-L5) becomes more electron-donating, in the order  $L5 > L4 > L1 > L3 > L2$ . The nature of the observed electronic spectra and the position of absorption bands are reliable with those of other similar octahedral ruthenium (II) complexes<sup>22</sup>. The higher energy bands observed in the UV region (242-292 nm) are of intraligand  $\pi-\pi^*$  type.

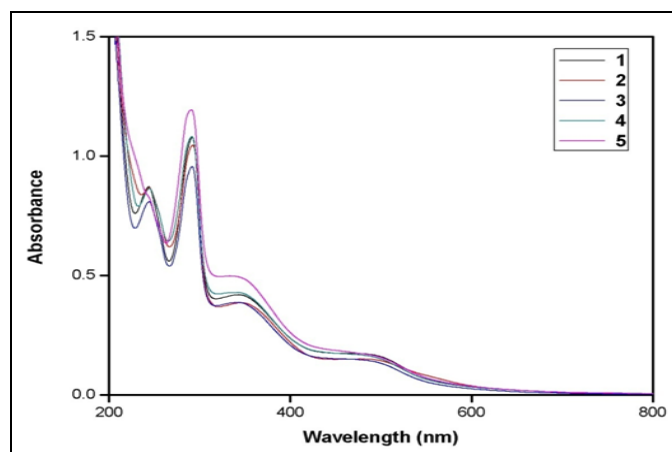


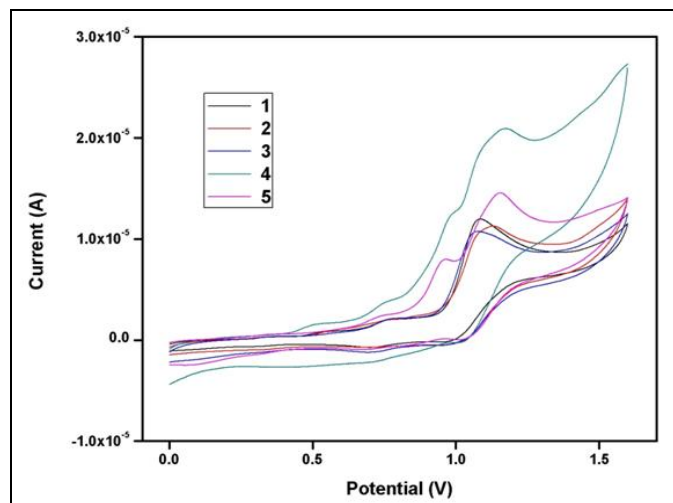
**FIG. 2 ELECTRONIC ABSORBANCE SPECTRA OF RUTHENIUM COMPLEXES IN ACETONITRILE**

The IR spectra of the complexes (1-5) contain many sharp bands of different intensities due to the vibrations arising from the coligands (L1-L5) and 2, 2'-bipyridine. The  $\nu_{\text{C=N}}$  stretching frequency of the free ligands (L1-L5) appears near  $1607 \text{ cm}^{-1}$  has been shifted to  $1602 \text{ cm}^{-1}$  in the present complexes in accordance with the coordination of the azomethine function to the metal ion<sup>23,24</sup>. In the IR spectra of all the ligands, a sharp band observed in the region of  $1506-1544 \text{ cm}^{-1}$  has been assigned to  $\nu_{\text{C=C}}$  stretching frequency. Upon coordination, these bands have been shifted around  $1516 \text{ cm}^{-1}$ , thereby indicating the coordination of the ligands with the ruthenium metal. The presence of a medium intensity band at  $744-844 \text{ cm}^{-1}$  in the ligands is characteristic of CH out-of-plane bending mode<sup>25</sup>.

The electrochemical features of the mononuclear ruthenium (II) complexes 1-5 were investigated in acetonitrile by employing cyclic voltammetry (CV) and differential pulse voltammetry (DPV) on a glassy carbon working electrode. Typical cyclic voltammograms of the present complexes is depicted in **Fig. 3**. The redox parameters of these complexes are listed in **Table 1**. The values of anodic peak potentials ( $E_{\text{pa}}$ ) indicate the energy required for oxidation of the central metal ion in the complex species, while the values of cathodic peak potential ( $E_{\text{pc}}$ ) indicate the energy required for reduction of the metal ion.

**TABLE 1: ELECTRONIC AND ELECTROCHEMICAL DATA OF MONONUCLEAR RUTHENIUM (II) COMPLEXES IN ACETONITRILE SOLUTION AT 25 ± 0.2 °C**

Complex	$\lambda_{\max}$ , nm ( $\epsilon$ , M <sup>-1</sup> cm <sup>-1</sup> )	$E_{p,a}$ (V)	$E_{p,c}$ (V)	$\Delta E_p$ (mV)	$E_{1/2}$ Ru <sup>II</sup> /Ru <sup>III</sup> vs SCE	
					CV (V)	DPV (V)
[Ru(bpy) <sub>2</sub> (L1)](PF <sub>6</sub> ) <sub>2</sub>	464 (8700) 343(20950) 290(53750) 242(43450)	1.0834	0.9749	108	1.0291	1.0198
[Ru(bpy) <sub>2</sub> (L2)](PF <sub>6</sub> ) <sub>2</sub>	462 (7400) 346(19350) 292(52350) 244(43400)	1.1092	0.9964	112	1.0528	1.0489
[Ru(bpy) <sub>2</sub> (L3)](PF <sub>6</sub> ) <sub>2</sub>	463 (7500) 338(19350) 291(47850) 242(40200)	1.0691	0.9931	76	1.0311	1.0342
[Ru(bpy) <sub>2</sub> (L4)](PF <sub>6</sub> ) <sub>2</sub>	466 (8550) 344(21450) 290(53900) 244(43250)	1.1194	1.0246	94	1.0720	1.0677
[Ru(bpy) <sub>2</sub> (L5)](PF <sub>6</sub> ) <sub>2</sub>	470 (8850) 332(24900) 289(59600) 245(41300)	1.1507	1.0074	143	1.0791	1.0731

**FIG. 3: CYCLICVOLTAMMOGRAMS OF RUTHENIUM COMPLEXES IN ACETONITRILE AGAINST SCE AT A SCAN RATE OF 100 MVS<sup>-1</sup>**

All the complexes exhibit a quasi-reversible metal-based oxidative response with  $E_{1/2}$  values falling in the range of +1.0291 - +1.0791 V. The peak potential separations  $\Delta E_p$  (76-143 mV) are generally larger than the ideal Nernstian value of 59 mV for a one-electron transfer, but commonly observed for complexes of this type apparently due to uncompensated solution resistance<sup>26</sup>. The Ru (II) / Ru (III) potentials follow the trend 5 > 4 > 2 > 3 > 1, which reflects the changes to the electronic environment around Ru (II) along with this series

upon varying the substituent in the ligand. The high Ru (II) / Ru (III) redox potentials of the present complexes may be due to the strong  $\pi$ -delocalization of benzimidazole based ligands. The redox potential of 1 has been observed at +1.0291 V with a peak separation of 108 mV. Whereas complexes 2 and 3 exhibited the redox peaks at +1.0528 and +1.0311 V, respectively.

Complex 5 showing a greater stabilization for the Ru (II) species could be related to the presence of methoxy group enhancing the  $\pi$ -acidity of the ligand. Further, the  $E_{1/2}$  values of the present complexes are lower than the analogous imidazole based complexes, which may be attributed to the electron withdrawing benzimidazole moiety present in the synthesized complexes<sup>22</sup>.

**DNA Cleavage Activity of Ruthenium (II) Complexes:** The agarose gel electrophoresis method was employed to monitor the degree of DNA cleavage by the newly synthesized compounds. No cleavage activity was observed in the absence of light **Fig. 4**. On the other hand, on irradiating the compounds in the presence of light at the wavelength of 480 nm, cleavage of supercoiled plasmid DNA has been observed even at a concentration of 24  $\mu$ M.

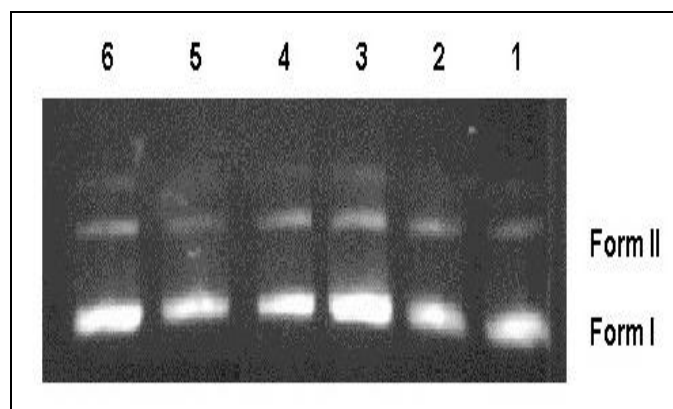


**FIG. 4: CLEAVAGE OF SUPERCOILED PUC19DNA BY THE COMPLEXES (1-5) IN THE ABSENCE OF LIGHT (LANE 2-6).** Lane 1: DNA alone; Lane 2: DNA+24  $\mu$ M complex 1; Lane 3: DNA+24  $\mu$ M complex 2; Lane 4: DNA+24  $\mu$ M complex 3; Lane 5: DNA+24  $\mu$ M complex 4; Lane 6: DNA+24  $\mu$ M complex 5

On increasing the concentration of the compounds to 48  $\mu$ M, complete cleavage of DNA has been observed **Fig. 5**. In order to find out the reactive species involved in the cleavage mechanism, a control experiment with DMSO (hydroxyl radical scavenger) and histidine (singlet oxygen quencher) has been carried out. In a reaction with DMSO (10 mM) no DNA cleavage has been observed, ruling out the possibility of DNA cleavage via OH-based depurination pathway and also a possible oxidative cleavage<sup>27, 28</sup>. While carrying out the reaction with histidine (10 mM), it has not been shown to exhibit any inhibitory effect in the DNA cleaving ability of the complexes **Fig. 6**. This clearly shows that the complexes cleave the DNA by direct guanine oxidation rather than through singlet oxygen.

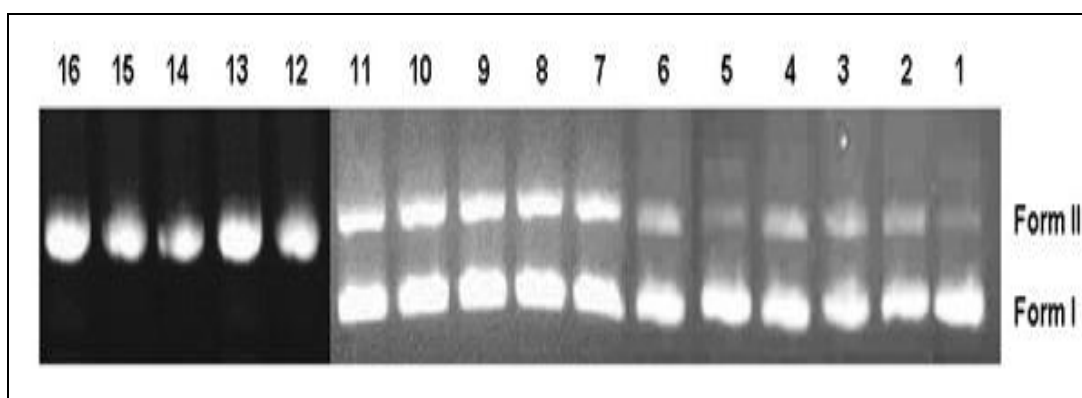


**FIG. 5: CLEAVAGE OF PUC19 DNA BY COMPLEXES (1-5) AT VARIOUS CONCENTRATIONS WHEN EXPOSED TO LIGHT AT 480 NM. DNA WAS INCUBATED WITH COMPLEX FOR 60 MIN IN TRIS BUFFER (PH 7.2) AT 37 °C.** Lane 1, DNA control Lane 2: DNA+12  $\mu$ M complex 1; Lane 3: DNA+12  $\mu$ M complex 2; Lane 4: DNA+12  $\mu$ M complex 3; Lane 5: DNA+12  $\mu$ M complex 4; Lane 6: DNA+12  $\mu$ M complex 5; Lane 7: DNA+24  $\mu$ M complex 1; Lane 8: DNA+24  $\mu$ M complex 2; Lane 9: DNA+24  $\mu$ M complex 3; Lane 10: DNA+24  $\mu$ M complex 4; Lane 11: DNA+24  $\mu$ M complex 5; Lane 12: DNA+48  $\mu$ M complex 1; Lane 13: DNA+48  $\mu$ M complex 2; Lane 14: DNA+48  $\mu$ M complex 3; Lane 15: DNA+48  $\mu$ M complex 4; Lane 16: DNA+48  $\mu$ M complex 5

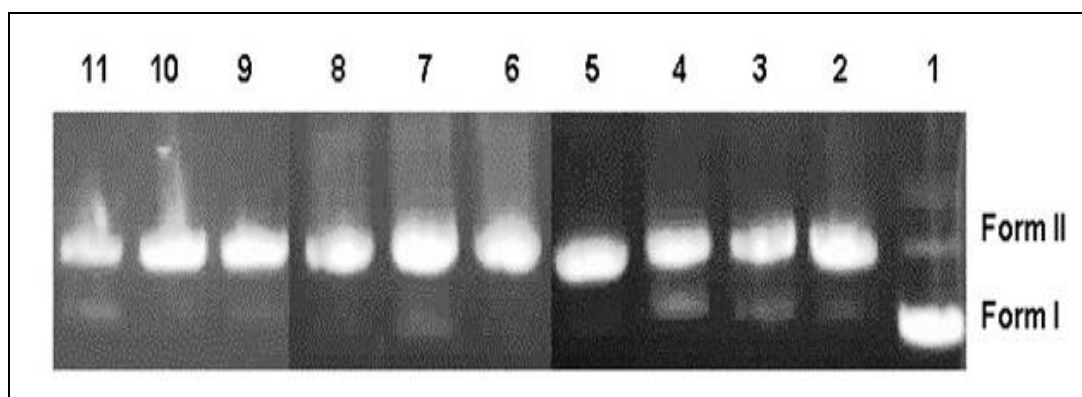


**FIG. 6: CLEAVAGE OF PUC19 DNA BY COMPLEXES (1-5) TO LIGHT AT 480 NM IN THE PRESENCE OF HISTIDINE AND DMSO. DNA WAS INCUBATED WITH COMPLEX FOR 60 MIN IN TRIS BUFFER (PH 7.2) AT 37°C.** Lane 1, DNA control; Lane 2, DNA + 1 (48  $\mu$ M) + Histidine (10 mM); Lane 3, DNA + 2 (48  $\mu$ M) + Histidine (10 mM); Lane 4, DNA + 3 (48  $\mu$ M) + Histidine (10 mM); Lane 5, DNA + 4 (48  $\mu$ M) + Histidine (10 mM); Lane 6, DNA + 5 (48  $\mu$ M) + Histidine (10 mM); Lane 7, DNA + 1 (48  $\mu$ M) + DMSO (10 mM); Lane 8, DNA + 2 (48  $\mu$ M) + DMSO (10 mM); Lane 9, DNA + 3 (48  $\mu$ M) + DMSO (10 mM); Lane 10, DNA + 4 (48  $\mu$ M) + DMSO (10 mM); Lane 11, DNA + 5 (48  $\mu$ M) + DMSO (10 mM)

**Antiproliferative Activity of Ruthenium (II) Complexes:** The present study examined the efficacy of ruthenium (II) complexes to inhibit the human breast cancer cell line (MCF-7) as determined by MTT assay. The cells were treated with five different concentrations ranging from 0.1 to 100  $\mu\text{M}$ . The complexes suppressed the growth of breast cancer cell lines in a dose-dependent manner. The maximum cell inhibitions of 100, 99.13, 98.72, 98.63 and 92.87% at 100  $\mu\text{M}$  concentration were determined for 1, 2, 4, 5 and 3 respectively and minimum inhibitions (-1.09, -0.82, 0.54, 1.1 and 2.60%) at 0.1  $\mu\text{M}$  concentration were observed for 3, 2, 4, 1 and 5 respectively **Fig. 7**.

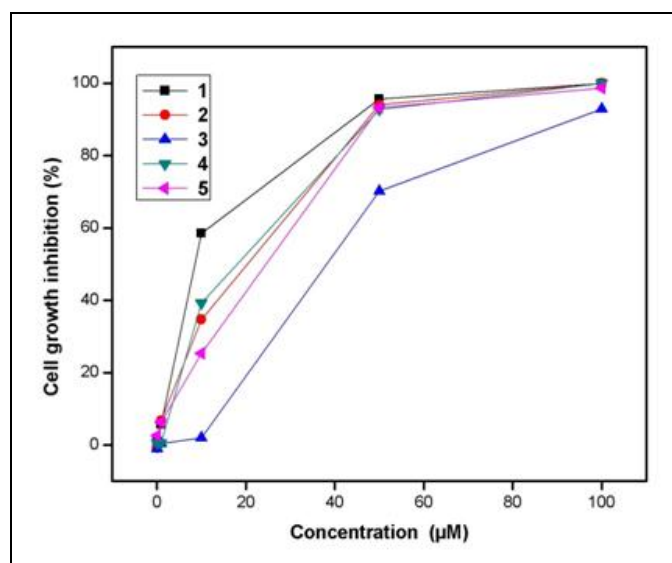


**FIG. 7: EFFECTS OF RUTHENIUM (II) COMPLEXES ON THE CELL GROWTH INHIBITION OF MCF-7 CELLS (HUMAN BREAST CANCER), FOLLOWING CONTINUOUS INCUBATION FOR 48 h, WITH INCREASING DRUG CONCENTRATION (0.1–100  $\mu\text{M}$ ). RESULTS ARE REPRESENTATIVE OF THREE INDEPENDENT EXPERIMENTS (N = 3)**

From the results presented in **Table 2**, it is clear that several ruthenium complexes exhibited a marked inhibitory effect on the proliferation of MCF-7 cancer cells. The  $\text{IC}_{50}$  values for complexes treated with MCF-7 cells were obtained at 7.9, 13.49, 36.78, 12.57, and 16.0  $\mu\text{M}$  for 1, 2, 3, 4, and 5, respectively.

Out of the five complexes tested,  $\text{IC}_{50}$  value for 1 is found to be less, suggesting that 1 could exert a very strong anti-proliferative effect when compared to other complexes tested with breast cancer cell lines at low doses. The complexes exhibited higher cytotoxic effects on breast cancer cells with lower

$\text{IC}_{50}$  values indicating their efficiency in killing the cancer cells even at low concentrations. There are reports in the literature on the cytotoxic effects of the complexes with longer incubation time periods<sup>29-31</sup>. The longer incubation period may result in the development of cellular resistance for that particular complex.

**TABLE 2: IN-VITRO CYTOTOXIC ACTIVITY OF SYNTHESIZED RUTHENIUM (II) COMPLEXES IN HUMAN BREAST CANCER CELL LINE (MCF7)**

S. no.	Compound	$\text{IC}_{50}$ value ( $\mu\text{M}$ )
1	[Ru(bpy) <sub>2</sub> (L1)](PF <sub>6</sub> ) <sub>2</sub>	7.9
2	[Ru(bpy) <sub>2</sub> (L2)](PF <sub>6</sub> ) <sub>2</sub>	13.49
3	[Ru(bpy) <sub>2</sub> (L3)](PF <sub>6</sub> ) <sub>2</sub>	16.78
4	[Ru(bpy) <sub>2</sub> (L4)](PF <sub>6</sub> ) <sub>2</sub>	12.57
5	[Ru(bpy) <sub>2</sub> (L5)](PF <sub>6</sub> ) <sub>2</sub>	16.0

### Biocidal Studies of Ruthenium (II) Complexes:

*In-vitro* antimicrobial activity of a test drug is measured in terms of zone of inhibition produced. The higher the diameter of the zone higher is the microbial growth inhibition.

The *in-vitro* antimicrobial screening of the ligands and complexes were carried out against *Staphylococcus aureus*, *Escherichia coli*, and *Candida albicans* by disc diffusion method<sup>32</sup>. From the results in **Table 3**, it has been observed that ruthenium complexes showed better activity than the free ligands.

This can be attributed to Tweedy's chelation theory<sup>33-35</sup>, according to which chelation reduces the polarity of the central metal atom mainly because of partial sharing of its positive charge with a donor group and possible  $\pi$ -electron delocalization taking place over the whole ring. This increases the lipophilic character of the metal chelate, which favors the permeation of the complexes through the lipid layer of the cell membrane.

The complexes possess activity, which is greater than the effectiveness of the standard drug, Gentamycin. It has been observed that the inhibition activity of the compounds increases with an increase in the concentration of the solution. The activity of the complexes against the microbes follows the order: *E. coli* > *S. aureus* > *C. albicans*. Moreover, the complexes are having pronounced antibacterial activity compared to antifungal activity.

TABLE 3: ANTIMICROBIAL ACTIVITY OF LIGANDS AND THEIR RUTHENIUM (II) COMPLEXES

S. no.	Test Drug	Zone of Inhibition (mm)								
		<i>S. aureus</i>			<i>E. coli</i>			<i>C. albicans</i>		
		25 µg/mL	50 µg/mL	100 µg/mL	25 µg/mL	50 µg/mL	100 µg/mL	25 µg/mL	50 µg/mL	100 µg/mL
1	L1	9	10	13	15	17	20	12	14	20
2	L2	10	13	15	12	15	19	11	12	15
3	L3	10	12	15	12	16	18	09	11	15
4	L4	9	11	14	13	16	19	11	13	16
5	L5	9	11	15	12	14	17	10	12	16
6	[Ru(bpy) <sub>2</sub> (L1)] (PF <sub>6</sub> ) <sub>2</sub>	21	24	31	17	22	30	15	18	26
7	[Ru(bpy) <sub>2</sub> (L2)] (PF <sub>6</sub> ) <sub>2</sub>	12	16	26	17	20	28	14	16	25
8	[Ru(bpy) <sub>2</sub> (L3)] (PF <sub>6</sub> ) <sub>2</sub>	15	20	30	16	20	25	14	16	22
9	[Ru(bpy) <sub>2</sub> (L4)] (PF <sub>6</sub> ) <sub>2</sub>	10	15	20	17	20	28	13	16	25
10	[Ru(bpy) <sub>2</sub> (L5)] (PF <sub>6</sub> ) <sub>2</sub>	11	16	27	16	18	30	18	20	26
11	Gentamycin Standard	-	-	16	-	-	16	-	-	-

Note: Zone size less than 15 mm – Least active; 16 – 20 mm – moderately active; Above 20 mm – highly active

**CONCLUSION:** The search for new molecular structures that exhibit effective antitumor activities is one of the most important goals of pharmacological research. This has driven inorganic chemists to look for new metal compounds with good activities, preferably against tumors that are responsible for high cancer mortality.

In this study, a new series of benzimidazole-based ruthenium (II) complexes were synthesized and characterized using various spectral techniques. The complexes are able to cleave supercoiled pUC19 plasmid DNA via guanine base oxidation in a concentration-dependent manner.

The cytotoxic studies showed that the complexes exhibit good cytotoxic activity against MCF-7 cancer cell lines. Furthermore, these complexes have potential practical applications to formulate into an efficient drug against cancer.

**ACKNOWLEDGEMENT:** We wish to thank SAIF-Cochin for carrying out elemental analysis. Also, SAIF-IITM is gratefully acknowledged for doing EI mass spectrometry. MK thanks UGC, New Delhi, India, for providing financial support in the form of MRP.

**CONFLICTS OF INTEREST:** The authors have no potential conflict of interest.

## REFERENCES:

- Zhang P and Sadler PJ: Redox-active Metal complexes for anticancer therapy. *European Journal of Inorganic Chemistry* 2017; 2(1): 1541-48.
- Rao ABP, Gulati K, Joshi N, Deb DK, Rambabu D, Kaminski W, Poluri KM and Kollipara MV: Synthesis and biological studies of ruthenium, rhodium and iridium metal complexes with pyrazole-based ligands displaying unpredicted bonding modes. *Inorganica Chimica Acta* 2017; 462(4): 223-35.
- Bergamo A and Sava G: Ruthenium anticancer compounds: Myths and realities of the emerging metal-based drugs. *Dalton Transactions* 2011; 40(31): 7817-23.
- Allardyce CS and Dyson PJ: Ruthenium in Medicine: current clinical uses and future prospects. *Platinum Metals Review* 2001; 45(2): 62-69.
- Lentzen O, Moucheron C and Kirsch-De Mesmaeker A: *Metallotherapeutic drugs and metal-based diagnostic agents*. John Wiley & Sons, Ltd: West Sussex 2005; 359.
- Ang WH, Casini A, Sava G and Dyson P: Organometallic ruthenium-based antitumor compounds with novel modes of action. *Journal of Organic Chemistry* 2011; 696(5): 989-98.
- Lentz F, Drescher A, Lindauer A, Henke M, Hilger RA, Hartinger GC, Scheulen ME, Dittrich C, Keppler BK and Jaehde U: Pharmacokinetics of a novel anticancer ruthenium complex (KP1019, FFC14A) in a phase I dose-escalation study. *Anti-Cancer Drugs* 2009; 20(2): 97-107.
- Galanski M, Arion VB, Jakupec MA and Keppler BK: Update of the pre-clinical situation of anticancer platinum complexes: novel design strategies and innovative analytical approaches. *Current Pharmaceutical Design* 2005; 12(18): 2075-94.
- Yan YK, Melchart M, Habtemariam A and Sadler PJ: Organometallic chemistry, biology and medicine: ruthenium arene anticancer complexes. *Chemical Communications* 2005; 14(38): 4764-76.
- Ang WH and Dyson PJ: Classical and non-classical ruthenium-based anticancer drugs: towards targeted

- chemotherapy. *European Journal of Inorganic Chemistry* 2006; 2006(20): 4003-18.
11. Gurer –Orhan H, Orhan H, Suzen S, Püsküllü MO and Buyukbingol E: Synthesis and evaluation of *in-vitro* antioxidant capacities of benzimidazole derivatives. *Journal of Enzyme Inhibition and Medicinal Chemistry* 2006; 21(2): 241-47.
  12. Ozkay Y, Tunai Y, Karaca H and Isikdag I: Antimicrobial activity and a SAR study of some novel benzimidazole derivatives bearing hydrazone moiety. *European Journal of Medicinal Chemistry* 2010; 45(8): 3293-3298.
  13. Zienab M, Nofal Elsyed A, Soliman SS, Abd El-Karim, Magdy I, Elzahar Aladdin M, Srouf SS and Timothy JM: Benzimidazoles: the latest information on biological activities. *Acta Poloniae Pharmaceutica. Drug Research* 2011; 68(1): 519-34.
  14. Periasamy M, Balasubramanian K and Chinnusamy V: Synthesis, characterization and biological activities of Ruthenium (II) Schiff base complexes. *Indian Journal of Chemistry* 2004; 43(10): 2132-36.
  15. Sathyaraj G, Kiruthika M, Weyhermuller T and Nair BU: Ruthenium (II) [3 + 2 + 1] mixed ligand complexes: substituent effect on photolability, photooxidation of bases, photocytotoxicity and photonuclease activity. *Dalton Transactions* 2012; 41: 8460-71.
  16. Sathyaraj G, Muthamilselvan D, Kiruthika M, Weyhermuller T and Nair BU: Ferrocene conjugated imidazolephenols as multichannel ditopic chemosensor for biologically active cations and anions. *Journal of Organometallic Chemistry* 2012; 716(12): 150-58.
  17. Hiort C, Lincoln P and Norden B: DNA binding of delta and lambda-[Ru(phen)2DPPZ]<sup>2+</sup>. *Journal of American Chemical Society* 1993; 115(9): 3448-54.
  18. Ahmad I and Beg AZ: Indian medicinal plants against multi-drug resistant human pathogens. *Journal of Ethnopharmacology* 2001; 74(2): 113-23.
  19. Andrews JM: Determination of minimum inhibitory concentrations. *Journal of Antimicrobial Chemotherapy* 2001; 49(6): 5-16.
  20. Mondal D, Pal P and Baitalik S: Anthraquinone-benzimidazole based ruthenium (II) complexes as selective multichannel anion sensors and multi-readout molecular logic gates and memory devices: Combined experimental and DFT/TD-DFT study. *Sensors and Actuators B: Chemical* 2017; 242(12): 746-59.
  21. Lever ABP: *Inorganic Electronic Spectroscopy*. Elsevier, Second edition, New York, 1984
  22. Kiruthika M and Dharmalingam P: Heteroleptic mononuclear ruthenium (II) complexes: synthesis, characterization, DNA cleavage, antioxidant and cytotoxic activities. *International Journal of Pharmaceutical Sciences and Research* 2017; 8(3): 1485-91.
  23. Rajput J, Moss JR, Hutton AT, Hendricks DT, Arendse CE and Imrie C: Synthesis, characterization and cytotoxicity of some palladium(II), platinum(II), rhodium(I) and iridium(I) complexes of ferrocenylpyridine and related ligands. Crystal and molecular structure of trans-dichlorobis (3-ferrocenylpyridine) palladium (II). *Journal of Organometallic Chemistry* 2004; 689(9): 1553-68.
  24. Balasubramanian KP, Raju VV and Chinnusamy V: Synthesis, characteristic, catalytic and antimicrobial activities of imidazole substituted benzilidene imines with ruthenium (II) complexes. *Journal of Indian Chemical Society* 2009; 86(6): 570-76.
  25. Arancibia R, Klahn AH, Buono-Core GE, Contreras D, Barriga G, Olea-Azar C, Lapiere M, Maya JD, Ibañez A and Garland MT: Organometallic Schiff bases derived from 5-nitrothiophene and 5-nitrofurane: Synthesis, crystallographic, electrochemical, ESR and anti-trypansomoma cruzi studies. *Journal of Organometallic Chemistry* 2013; 743(6): 49-54.
  26. Karvembu R, Hemalatha S, Prabhakaran R and Natarajan K: Synthesis, characterization and catalytic activities of ruthenium complexes containing triphenylphosphine / triphenylarsine and tetra dentate Schiff bases. *Inorganic Chemistry Communications* 2003; 6(5): 486-90.
  27. Reddy PR, Shilpa A, Raju N and Raghavaiah P: Synthesis, structure, DNA binding and cleavage properties of ternary amino acid Schiff base-phen/bipy Cu(II) complexes. *Journal of Inorganic Biochem* 2011; 105(12): 1603-12.
  28. Riha M, Karlickova J, Filipovsky T and Macakova K: Novel method for rapid copper chelation assessment confirmed low affinity of D-penicillamine for copper in comparison with trientine and 8-hydroxyquinolines. *Journal of Inorganic Biochemistry* 2013; 123: 80-87.
  29. Gao E, Sun Y, Liu Q and Duan L: An anticancer metallobenzylmalonate: crystal structure and anticancer activity of a palladium complex of 2, 2'-bipyridine and benzylmalonate. *Journal of Coordination Chemistry* 2006; 59(11): 1295-00.
  30. Ferrari M, Fornasiero MC and Isetta AM: MTT colorimetric assay for testing macrophage cytotoxic activity *in vitro*. *Journal of Immunological Methods* 1990; 131(90): 165-72.
  31. Rey NA, Neves A and Silva PP: A synthetic dinuclear copper(II) hydrolase and its potential as anti-tumoral: cytotoxicity, cellular uptake and DNA cleavage. *Journal of Inorganic Biochemistry* 2009; 103(10): 1323-30.
  32. Keyvan P, Leila B, Zahra R, Manuchehr S and Kamiar Z: *In-vitro* activity of six antifungal drugs against clinically important dermatophytes. *Jundishapur Journal of Microbiology* 2009; 4(3): 158-63.
  33. Vora J, Vasava S, Parmar K, Chauhan S and Sharma S: Synthesis, spectral and microbial studies of some novel Schiff base derivatives of 4-methylpyridin-2-amine. *E-Journal of Chemistry* 2009; 6(12): 1205-10.
  34. Bhalodia NR and Shukla V: Antibacterial and antifungal activities from leaf extracts of *Cassia fistula* L. an ethnomedicinal plant. *Journal of Advanced Pharmaceutical Technology and Research* 2011; 2(2): 104-09.
  35. Chakraborty B, Bhattacharyya UK and Nandy S: Study of antimicrobial activity of methanolic extract of *Alangium lamarkii* leaves against selected microbial species. *Int Journal of Pharma and Life Sciences* 2012; 3(4): 1620-23.

**How to cite this article:**

Kiruthika M, Elayaperumal R and Hariharan C: Synthesis, characterization and biological studies of ruthenium (ii) complexes of substituted 2-{4, 5-bis[(e)-2-phenylethenyl]-1h-imidazol-2-yl}-1h-benzimidazole. *Int J Pharm Sci & Res* 2020; 11(12): 6550-60. doi: 10.13040/IJPSR.0975-8232.11(12).6550-60.